THE JOURNAL OF PHYSICAL CHEMISTRY C

Article

pubs.acs.org/JPCC

Distinguishing Amorphous and Crystalline Ice by Ultralow Energy Collisions of Reactive Ions

Soumabha Bag, Radha Gobinda Bhuin, and T. Pradeep*

DST Unit of Nanoscience (DST UNS), Department of Chemistry, Indian Institute of Technology Madras, Chennai-600036, India

Supporting Information

ABSTRACT: Ion scattering using ultralow energy projectiles is considered to be a unique method to probe the nature of molecular surfaces because of its capacity to probe the very top, atomically thin layers. Here, we examine one of the most studied molecular solids, water-ice, using this technique. When ice surface undergoes the amorphous to crystalline transition, an ultralow energy reactive projectile identifies the change through the reaction product formed. It is shown that ultralow energy (2, 3, 4, 5, 6, and 7 eV) CH_2^+ (or CD_2^+) collision on amorphous D_2O (or H_2O) ice makes CHD^+, while crystalline ice does not. The projectile undergoes H/D exchange with the dangling −OD (−OH) bond present on amorphous ice surfaces. It is also shown that H/D exchange product disappears when amorphous ice is annealed to the crystalline phase. The H/D exchange reaction is shown to be sensitive only to the surface layers of ice as it disappears when the surface is covered with long chain alcohols like 1-pentanol as the ice surfaces become inaccessible for the incoming projectile. This article shows that ultralow energy reactive ion collision is a novel method to distinguish phase transitions in molecular solids.

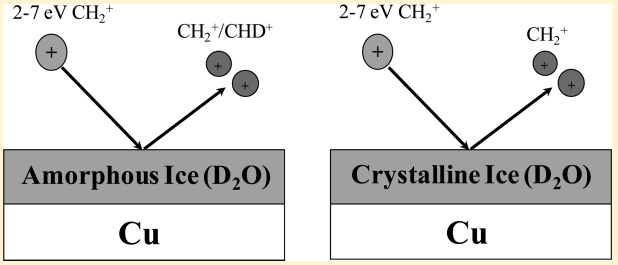

INTRODUCTION

Deposition of water vapor on cold surfaces creates two distinctly different forms of ice, amorphous and crystalline analogues where the former has more than one variety.[1,2] Distinction of these forms is important to conduct model studies as both the amorphous and the crystalline forms have unique chemical and physical properties. Since its first report in 1935, there have been numerous studies on the amorphous form of water.[3−5] While distinction of amorphous solid water (ASW) and crystalline water (CW) is possible by X-ray diffraction,[3] the most common tool for differentiation is infrared spectroscopy.[5−18] Structural differentiation is possible by other methods such as TPD,[13,19] LEED,[20] electron diffraction,[21] and TEM.[11] However, this differentiation must be made at the very top layer as it is the one that accommodates gaseous species of atmospheric relevance. Various ion scattering processes are used to understand molecular solids, in general,[22] and water ice, in particular, and these methods are summarized elsewhere.[23,24]

Low energy ion scattering is a unique tool for surface characterization, especially for molecular surfaces. Reactive collisions can distinguish adsorption geometry as well as the molecular nature of the collision partner. Ions at extremely low energy, of the order of few tens of electronvolt or less, are sensitive to the very top of molecular films,[25] especially the first chemical bond at the vacuum−surface interface. The ion scattering yield varies with the nature of the surfaces, and surface structure differentiation is possible from scattering yield measurements.[26] Such changes are due to the difference in the extent of neutralization, trapping, and accommodation. However, reactive collision in which the scattered ion undergoes chemical transformation by abstraction,[27] exchange,[28] or dissociation[29−33] can also be characteristic of the structure of the surface. When the ion energy is low, of the order of a few electronvolt, this collision event is extremely surface sensitive to the very first chemical bond of the air/vacuum−surface interface and therefore can distinguish structure, specific to the top layers.[25] Ion/surface collisions in the low energy regime need not always be reactive, and such processes have been used to characterize molecular diffusion,[34] nature of surface species,[35] and surface transformations.[36] For example, we have found a new surface transformation at ∼110 K for ASW, and this transformation is noticeable in a film of six or more monolayers of ice. While scattering events have been shown to be sensitive to the nature of the surface (amorphous/crystalline), there has been no report of distinguishing them by reactions.

In this work, we show that exchange reactions of specific ions can distinguish amorphous and crystalline ice. Such reactions occurring under 10 eV are specific to the first chemical bond, and therefore the information derived is unique in comparison to other techniques described earlier. Variation of reactive ions, easily achievable in mass spectrometry, can be used for such structural distinction for other ice. As ion doses are low in this static experiment, the properties of the surfaces can be retained even after prolonged periods of irradiation.[37−40]

Received: February 15, 2013
Revised: May 11, 2013
Published: May 20, 2013

   dx.doi.org/10.1021/jp4016432 | J. Phys. Chem. C 2013, 117, 12146−12152

EXPERIMENTAL SECTION

The instrumental setup and an outline of the experimental procedures are given elsewhere.[34,35] The low energy collision experiments and the precautions used were described earlier.[36] Briefly, the experiments described here were conducted in a double-chamber ultrahigh vacuum (UHV) system with a base pressure of $<5.0 \times 10^{-10}$ mbar. Each region of the system is pumped by a Pfeiffer Vacuum (TMU 261) 210 L/s turbomolecular drag pump. These two pumps are backed by another Pfeiffer Vacuum (TMU 071P) 60 L/s turbomolecular pump, which is further backed by a Pfeiffer Vacuum (MVP 055) 3.3 m^3/h dry pump. The electron impact (EI) source from ABB Extrel was used to generate positive ions. These ions are extracted from the source and transferred into a quadrupole mass filter (Q1) through a set of einzel lenses. Ion kinetic energy was controlled by varying the ion source conditions and tuning the rest of the optics. The scattered ions are detected by another quadrupole (Q3). All of the quadrupoles and control electronics are from Extrel Core Mass Spectrometry.

A high-precision UHV specimen translator with *xyz* axis movement and tilt was used. Polycrystalline copper was used as in previous experiments as the substrate for preparing amorphous and crystalline ice films.[27,41] Substrate plays a crucial role in determining the quality of the grown film. Yet, in the present case, the substrate effect is negligible due to higher coverages used. It may be noted that the dewetting temperature is much higher (~160 K) for 50 monolayer (ML) ice films.[42] The ice film grown at 120 K in ultrahigh vacuum is known to be amorphous in nature and of low porosity, while deposition above 140 K results in crystalline ice (CW).[43] The ice surface is prepared by exposing the cold substrate to water vapor at a specific pressure as described below.

The copper surface was grounded in all of the experiments. By varying the potential of the ion source block and tuning the rest of the ion optics, it was possible to produce a beam current of 1−2 nA for the mass selected ions. Various ions collide with the surface at an angle of 45° with reference to the surface normal, and the scattered ions were analyzed by a second quadrupole. The ions in the entire scattering region feel the same potential, and the einzel lenses on either side of the target surface are nearly at the same potential. Thus, the ions are subjected to a field free condition around the scattering center. Scattering geometry is such that ions do not make a glancing impact. The ion kinetic energy spread is largest at 1 eV, but reduces significantly at higher energies.

Required projectiles were generated by ionizing CH_4 (or CD_4 to produce CD_3^+ and CD_2^+) by electron impact and subsequently selecting the desired ions through quadrupole mass analyzer. CD_4 was purchased from Aldrich. The liquids used in our study (H_2O, deionized water after triple distillation, D_2O, and 1-pentanol) were purified by many freeze−pump−thaw cycles, before use. D_2O (99.96% D isotopic purity) and 1-pentanol were purchased from Aldrich. Molecular surfaces were prepared by depositing the corresponding vapors and were delivered very close to the substrate through a tube. The exposure was controlled by a leak valve. The gas-line was pumped thoroughly by a rotary pump to avoid impurities and contamination. The distance between the gas delivery tube and polycrystalline copper substrate was adjusted to obtain uniform sample growth on the substrate. This was confirmed by our previous experiments. When *n*-butanol (A) was deposited on water ice (B), water molecules could not diffuse through *n*-butanol layers at 120 and 140 K and get detected.[44] This observation confirms that the entire area under investigation had uniform growth of A over B. Nonuniform coverages would have made B to get detected. Delivery of molecules near the substrate ensured that the vapors were not deposited in unwanted areas. The deposition flux of the vapors was adjusted to ~0.1 ML/s. The thickness of the overlayers was estimated assuming that 1.33×10^{-6} mbar/s = 1 ML. The 1 ML ice layers have been estimated to contain $\sim 1.1 \times 10^{15}$ water molecules/cm^2.[45] In all of our experiments with ASW, the deposition temperature was kept at 120 K, which is known to grow ASW films.[46] The pressure(s) of the gas(es) inside the scattering chamber during deposition was 1×10^{-7} mbar. The films were prepared on polycrystalline Cu substrate to make Cu@A (the symbolism implies the creation of a layer of A over Cu). The film thickness was large so that the underlying Cu did not have any effect on the ice layer formed. The spectra presented here were averaged for 75 scans, and the data acquisition time was approximately 0.5 s per scan. The present instrumental setup does not allow temperature programmed desorption (TPD) measurements.

RESULTS

To check the distribution of ion kinetic energy (K.E.) of the input beam, stopping potential measurement was performed at Q1. In this measurement, Q1 was kept in the RF (radio frequency)-only mode where it transmits all ions formed in the source, and Q3 was set to transmit the desired mass. Thereafter, a range of DC voltages are applied across the quadrupoles to stop the desired ions. When the ions are stopped at Q1, for example, the intensity of the ions falls to zero. Figure 1 shows the results of stopping potential

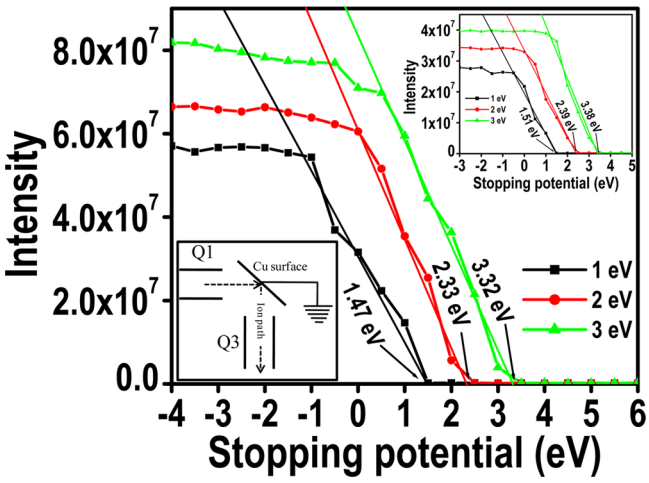

Figure 1. Plot of CH_2^+ stopping potential data at quadrupole 1 (Q1). Results of a similar kind of stopping potential measurement performed with quadrupole 3 (Q3) are shown in the inset. The experimental scheme is shown at the bottom left.

measurements of 1, 2, and 3 eV CH_2^+ ions. It is evident from the figure that for 1 eV ion, the energy spread is 47%, which reduces substantially (10%) in the case of 3 eV ions. With further increase in the input ion kinetic energy up to 8 eV, the spread decreases to 2% (data not shown). It is important to note that this kind of ion energy spread is the best that has been achieved so far in such instrumentation.[23] Increased spread at extremely low energy (1 eV) has been noted before.[36] Stopping

dx.doi.org/10.1021/jp4016432 | J. Phys. Chem. C 2013, 117, 12146−12152

potential measurement in Q3 using CH_2^+ (Q1 was set to select the desired ion and Q3 was kept as RF-only mode) showed little increase in energy spread in comparison to the stopping potential data of Q1. Similar stopping potential experiment using CH_3^+ and CH_4^+ revealed that other ions also followed a similar trend (Supporting Information, item numbers 1 and 2). The exchange experiment can be done with other ions too, but with CH_3^+ being a closed shell ion, exchange is not facile. In the case of CH^+, primary ion beam intensity was too low for low energy ion scattering experiments.

Having established the ion kinetic energy distribution, we performed ion scattering experiments to distinguish the nature of the surfaces. In Figure 2a, 2 eV CH_2^+ ion scattering spectrum

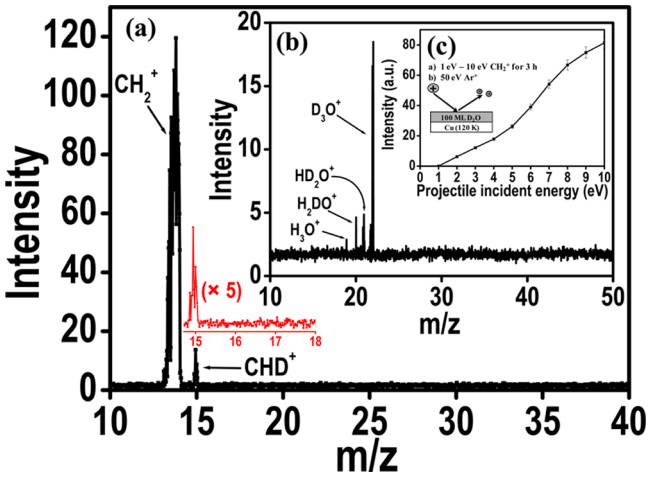

Figure 2. (a) Ion scattering mass spectrum of 2 eV CH_2^+ collision on amorphous D_2O at 120 K. The CHD^+ signal at m/z 15 is also shown separately in red with 5 times intensity enhancement. (b) Chemical sputtering spectra upon 50 eV Ar^+ impact on D_2O surfaces, irradiated with 1−10 eV CH_2^+ for 3 h. (c) The CHD^+ signal intensity with respect to increasing incident energy of CH_2^+. The experimental scheme is shown as an inset.

of D_2O prepared at 120 K is shown where m/z 14 is due to CH_2^+, the incident projectile, while the new peak at m/z 15 is assigned to CHD^+, the H/D exchange product. We have ensured that it is not due to CH_3^+ by conducting CD_2^+ collisions on H_2O (to be discussed later). Scattering experiments using other energy projectiles were also performed. After these experiments, chemical sputtering[47−49] experiments were performed using 50 eV Ar^+. The result is shown in Figure 2b. Peaks at m/z 19, 20, 21, and 22 are assigned to H_3O^+, H_2DO^+, HD_2O^+, and D_3O^+, respectively. This spectrum indicates that all of the H/D exchange products remain present on the surfaces. It may be noted that no such exchange products were seen on the parent D_2O ice surfaces. It also explains that H/D exchange has taken place due to the collision of CH_2^+ with amorphous ice (D_2O). Additionally, Figure 2c presents the normalized intensity plot of CHD^+ signal with respect to increasing CH_2^+ incident energy. This spectrum shows the formation of more CHD^+ as the kinetic energy of CH_2^+ increases.

In the next set of experiments, CH_2^+ was subjected to collisions on crystalline ice (D_2O), generated at 140 K (this temperature was chosen because it is known to give crystalline ice[46,50]). The results of those experiments are shown in Figure 3. It is evident from the figure that CHD^+ signals are absent. However, in this case, also H/D exchange takes place when

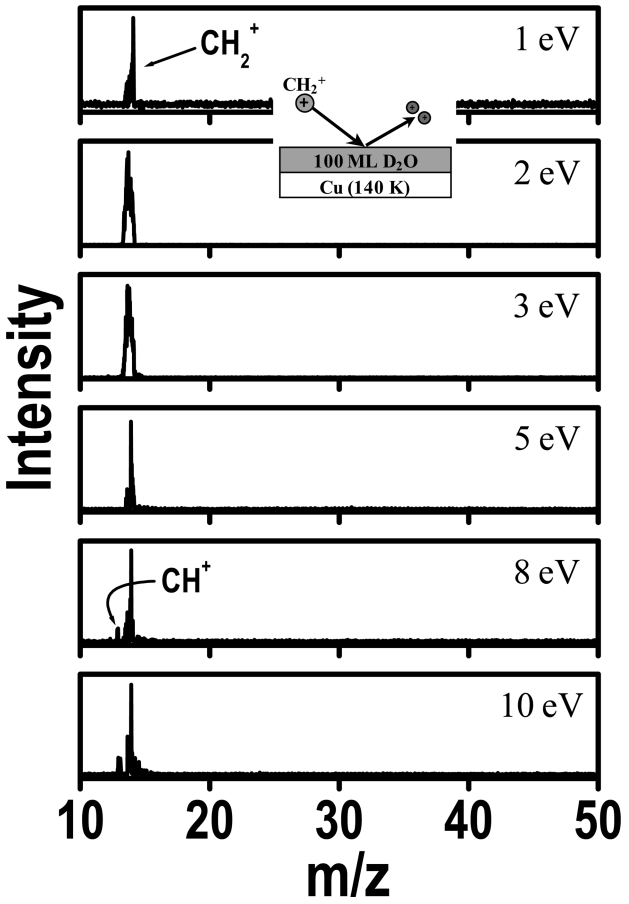

Figure 3. Mass spectra observed upon collisions of varying energy CH_2^+ on 100 ML crystalline ice (D_2O), generated at 140 K.

CH_2^+ ion energy is raised to ∼8 eV. At this energy, fragmentation of CH_2^+ occurs, and fragments, such as CH^+, are believed to react at the surfaces. For further understanding, the CH_2^+ projectiles were replaced with CD_2^+ and were subjected to collide on amorphous ice (generated upon condensing H_2O vapor at 120 K). The exchange product, CHD^+, was observed here also. Subsequently, chemical sputtering experiments were performed on the reacted surfaces. The results are shown in Figure 4. All of the possible H/D exchange products appeared in the sputtering spectrum. When the CHD^+ signal intensity was plotted with increasing CD_2^+ kinetic energy (inset of Figure 4), it showed a shape similar to that of CHD^+ (upon CH_2^+ collision with increasing kinetic energy, Figure 2c). These results confirm that H/D exchange occurs on amorphous ice by ultralow energy reactive projectiles like CH_2^+/CD_2^+ (on D_2O/H_2O).

To understand the difference in reactivity of CH_2^+ on amorphous and crystalline ice, a control experiment was performed at a lower projectile ion flux than the previous experiments (so as to avoid ion-induced surface damage, although insignificant at this energy range). At first, ultralow energy CH_2^+ was subjected to collide on amorphous ice (D_2O), and then the ice layer was annealed at 140 K to make it crystalline. Figure 5 shows the results of an ultralow energy ion scattering experiment performed on amorphous ice. As is evident in the spectra, the H/D exchange is observable by the appearance of CHD^+ signal at 2 eV. At higher energy (8 eV and above) surface-induced dissociation of the projectile led to the generation of various other signals. This experiment was carried

dx.doi.org/10.1021/jp4016432 | J. Phys. Chem. C 2013, 117, 12146−12152

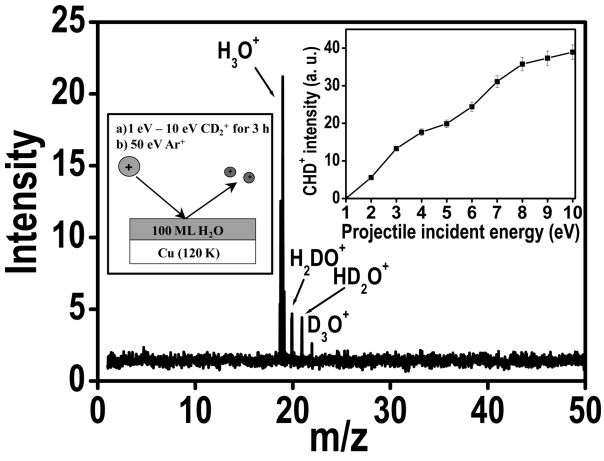

Figure 4. Chemical sputtering spectra observed with 50 eV Ar^+ on reacted amorphous ice (H_2O) formed after impact of 1−10 eV CD_2^+ for 3 h. CHD^+ signal intensity with increasing energy CD_2^+ is shown in one inset. Schematic presentation of the experiments is shown in another inset.

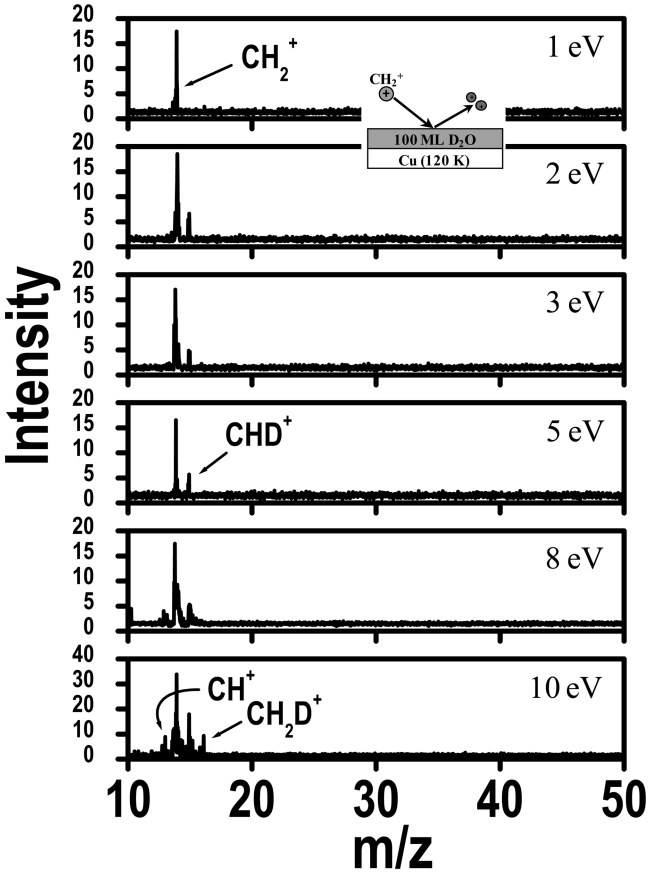

Figure 5. Ion scattering spectra observed upon collision of 1, 2, 3, 5, 8, and 10 eV CH_2^+ on amorphous ice (D_2O). Schematic presentation of the experiment is shown in the inset.

out again by annealing the underlying ASW to CW. After that, when the same experiment was carried out at the same energy window on CW, no H/D exchange was found below 8 eV energy (see Supporting Information, item number 4). The reason is believed to be the chemical reactivity difference between amorphous and crystalline ice surfaces with the incoming projectile. The presence of free hydroxyl bonds on ASW makes the H/D exchange possible with CH_2^+, and, consequently, the product CHD^+ appears. However, there may be other effects also that contribute to the chemical reactivity of the two surfaces (see below). No observable H/D exchange take place upon collision of CH_2^+ on crystalline ice surfaces. However, at a collision energy 8 eV and above, the reactive projectile starts breaking down on the surface of ice, and it generates fragmented products, which can make additional reactions. So, reactive collision at this energy region is not suitable to distinguish ASW and CW. To confirm the process of formation of CHD^+, 50 ML amorphous ice (D_2O) surface was covered with 200 ML 1-pentanol. After that, ultralow energy CH_2^+ was collided on it. Supporting Information item number 5 shows the scattered ion mass spectra observed upon collision of 1, 2, 3, 5, 8, 10 eV CH_2^+ on the condensed 1-pentanol overlayer. It is evident from the spectra that the H/D exchange product CHD^+ is absent. After the ultralow energy collision of CH_2^+, chemical sputtering experiment was performed using 50 eV Ar^+. The inset of Supporting Information item number 5 shows the resultant mass spectrum. The spectra resemble normal chemical sputtering spectra of 1-pentanol. The observation can be explained based on the following results. On 200 ML 1-pentanol covered amorphous ice, reactive collisions of ultralow energy CH_2^+ did not yield any H/D exchange, and no CHD^+ signal appeared during the ultralow energy ion scattering experiment. Additionally, CH_2^+ did not trigger any H/D exchange on 1-pentanol ice itself. Therefore, it may be concluded that the amorphous ice surfaces (D_2O) are responsible for H/D exchange in the projectile; when amorphous ice becomes inaccessible for the projectile (CH_2^+) due to the 1-pentanol overlayer, H/D exchange product does not appear.

DISCUSSION

The study of stopping potential measurement revealed that CH_2^+, CH_3^+, and CH_4^+ follow a similar trend (Figure 1, Supporting Information, item numbers 1 and 2). The stopping potential experiments at Q3 showed that the ion kinetic energy decreases slightly after colliding with the substrate (see Figure 1, inset). The reason for choosing low energy CH_2^+ over CH_3^+ and CH_4^+ is the following. CH_3^+ could not be used as it is a closed shell ion, and hence its reactivity is very low toward water molecules. CH_2^+ (or CD_2^+) and CH_4^+ (or CD_4^+) are suitable ions for the purpose of this reaction as these are open shell ions. CH_4^+ was discarded as it did not produce CH_3D^+ at low energy; instead, it started breaking down on the ice surfaces beyond 5 eV (Supporting Information, item number 3). All of the aforementioned ions undergo thermoneutral reactions with water ice surfaces. When CH_2^+ was allowed to impinge on D_2O, the H/D exchange product CHD^+ was seen. On the other hand, this product is not observed during collision on crystalline ice surfaces.

Results indicate that there are differences in chemical reactivity between amorphous and crystalline ice surfaces as mentioned before. There may be several effects that can affect the change in reactivity of the surfaces in microscopic detail, which include the difference in population of free hydroxyl groups on the two ice surfaces, dewetting,[20,51−56] film morphology change due to collapse of pores,[57] etc. Crystallization-induced dewetting is unlikely to be playing any role in this case as ice films are thick.[36,58] Dewetting of ice films grown on Cu(111) occurs around 160 K for a 50 ML film,[36] and dewetting temperature increases with film thickness.[56]

dx.doi.org/10.1021/jp4016432 | J. Phys. Chem. C 2013, 117, 12146−12152

Note that our experiment is on 100 ML films conducted at 140 K. Morphology change due to the collapse of pores will not contribute at 140 K as the pores collapse near ∼118 K.[59] In view of these facts, it is likely that free hydroxyl groups present on the ice surfaces are responsible for the reactivity change. Shen and colleagues reported coverage of dangling hydroxyl groups on the liquid water−air interface to be one-quarter of the available OH bonds.[19,60] Amorphous ice surfaces have a large number of dangling hydroxyl groups exposed to vacuum.[57,61,62] This population on the surfaces reduces when the amorphous ice is annealed to the crystalline form due to massive reconstruction that takes place during phase transition.[61] It may be noted that the absorbances of dangling hydroxyl bands decrease to near zero values around 140 K.[57] Thus, due to the large population of free hydroxyl groups on the amorphous ice surfaces, a larger extent of H/D exchange reactions occur here. On crystalline ice, the reaction does not occur to the same extent, and CHD^+ is not detected. However, the formation of CHD^+ is not ruled out as crystalline ice surfaces also possess free hydroxyl groups on its surfaces. Probably, the signal intensity is below the limit of detection in the case of CW. The reaction is proposed to proceed as $CH_2^+ + D_2O \rightarrow CHD^+ + HOD$, where CH_2^+ and CHD^+ are the gas-phase species and are detected by the mass spectrometer. Exchange reaction is a thermoneutral process. With increase in CH_2^+ kinetic energy, the H/D exchange product intensity increases (Figure 2c). Two factors are mainly responsible for this. First, scattering intensity increases with the increase in incident ion kinetic energy. Second, above 8 eV kinetic energy, the projectiles were fragmented on ice surfaces, and the products opened another path for more H/D exchange. This also contributed to the enhancement of the intensity of the CHD^+ ion. To establish this reason, ASW layers were prepared, onto which ultralow energy CH_2^+ were subjected to collide. This collision results in normal H/D exchange due to the presence of a large number of dangling −OD bonds on the surfaces (Figure 5) as mentioned above. After that, when the ASW was transformed to CW by annealing at 140 K, the same ultralow energy projectile did not cause detectable H/D exchange (Supporting Information, item number 4) product. The role of ASW in the reactive collision was confirmed by another investigation. First, 50 ML ASW (D_2O) layer was developed on Cu followed by 200 ML 1-pentanol layer. 200 ML thick 1-pentanol ensured that no D_2O molecules diffuse through the 1-pentanol layers and appear on the surface. On this sandwich surface, when the ultralow energy CH_2^+ was impinged, no CHD^+ signal was found. It is concluded that due to the presence of solid 1-pentanol cover, reactive CH_2^+ could not interact with the dangling −OD of the ASW (D_2O). Hence, no H/D exchange product appeared. This was again confirmed by 50 eV Ar^+ sputtering spectra (inset of Supporting Information, item number 5). The mass spectra consist of peaks, which originate from the sputtering of 1-pentanol. These control experiments confirm that the H/D exchange originated from the interaction of ASW (D_2O) surfaces with ultralow energy projectile (CH_2^+). Whenever the ASW surface was modified or covered, low energy H/D exchange did not take place. It can be further confirmed that this kind of ultralow energy reactive scattering is extremely surface sensitive particularly in the projectile kinetic energy range of 2−7 eV.

SUMMARY

This work shows that reactive projectiles of low energy react differently with structurally different surfaces. CH_2^+ with energy in the range 2−7 eV are suitable in differentiating the nature of ice surfaces. ASW (D_2O) surfaces have dangling −OD groups with which CH_2^+ reacts and undergoes H/D exchange to yield CHD^+. Dangling −OD groups population on the surfaces exposed to vacuum are very low on CW (D_2O); therefore, CH_2^+ collisions with this kind of surfaces do not produce any observable H/D exchange. Different experiments discussed in this Article describe a suitable method to distinguish ASW from CW with ultrahigh surface specificity.

ASSOCIATED CONTENT

Supporting Information

(1) Stopping potential experiment of CH_3^+ performed at Q1, (2) stopping potential experiment of CH_4^+ performed at Q1, (3) mass spectra observed upon collision with varying energy of CH_4^+ on 100 ML ASW (D_2O) generated at 120 K, (4) mass spectra observed after collision of varying energy CH_2^+ projectile on crystalline ice (D_2O), which was made after annealing the amorphous ice layer, and (5) mass spectra recorded upon collision of CH_2^+ impinging at 1, 2, 3, 5, 8, and 10 eV kinetic energy. Inset shows sputtering spectra appeared upon the collision of 50 eV Ar^+ on the substrate. This material is available free of charge via the Internet at http://pubs.acs.org.

AUTHOR INFORMATION

Corresponding Author

*Fax: + 91-44 2257-0545. E-mail: pradeep@iitm.ac.in.

Notes

The authors declare no competing financial interest.

ACKNOWLEDGMENTS

T.P. acknowledges the Department of Science and Technology, Government of India, for funding through a Swarnajayanti fellowship. He also thanks the DST for continued support. S.B. and R.G.B. acknowledge the Council of Scientific and Industrial Research (CSIR), Government of India, for their research fellowships.

REFERENCES

(1) Tribello, G. A.; Slater, B.; Salzmann, C. G. A Blind Structure Prediction of Ice XIV. *J. Am. Chem. Soc.* **2006**, *128*, 12594−12595.
(2) Lobban, C.; Finney, J. L.; Kuhs, W. F. The Structure of a New Phase of Ice. *Nature* **1998**, *391*, 268−270.
(3) Burton, E. F.; Oliver, W. F. X-ray Diffraction Patterns of Ice. *Nature* **1935**, *135*, 505−506.
(4) Angell, C. A. Amorphous Water. *Annu. Rev. Phys. Chem.* **2004**, *55*, 559−583.
(5) Olander, D. S.; Rice, S. A. Preparation of Amorphous Solid Water. *Proc. Natl. Acad. Sci. U.S.A.* **1972**, *69*, 98−100.
(6) Callen, B. W.; Griffiths, K.; Norton, P. R. Observation of Free Hydroxyl Groups on the Surface of Ultra Thin Ice Layers on Ni(110). *Surf. Sci.* **1992**, *261*, L44−L48.
(7) Devlin, J. P.; Buch, V. Vibrational Spectroscopy and Modeling of the Surface and Subsurface of Ice and of Ice-Adsorbate Interactions. *J. Phys. Chem. B* **1997**, *101*, 6095−6098.
(8) Delzeit, L.; Powell, K.; Uras, N.; Devlin, J. P. Ice Surface Reactions with Acids and Bases. *J. Phys. Chem. B* **1997**, *101*, 2327−2332.
(9) Devlin, J. P.; Joyce, C.; Buch, V. Infrared Spectra and Structures of Large Water Clusters. *J. Phys. Chem. A* **2000**, *104*, 1974−1977.

(10) Rowland, B.; Kadagathur, N. S.; Devlin, J. P.; Buch, V.; Feldman, T.; Wojcik, M. J. Infrared Spectra of Ice Surfaces and Assignment of Surface-Localized Modes from Simulated Spectra of Cubic Ice. *J. Chem. Phys.* **1995**, *102*, 8328−8341.
(11) Jenniskens, P.; Banham, S. F.; Blake, D. F.; McCoustra, M. R. S. Liquid Water in the Domain of Cubic Crystalline Ice I_c. *J. Chem. Phys.* **1997**, *107*, 1232−1241.
(12) Buontempo, U. Infrared Spectra of Amorphous Ice. *Phys. Lett. A* **1972**, *42*, 17−18.
(13) Bolina, A. S.; Wolff, A. J.; Brown, W. A. Reflection Absorption Infrared Spectroscopy and Temperature-Programmed Desorption Studies of the Adsorption and Desorption of Amorphous and Crystalline Water on a Graphite Surface. *J. Phys. Chem. B* **2005**, *109*, 16836−16845.
(14) Buch, V.; Milet, A.; Vacha, R.; Jungwirth, P.; Devlin, J. P. Water Surface Is Acidic. *Proc. Natl. Acad. Sci. U.S.A.* **2007**, *104*, 7342−7347.
(15) Mate, B.; Medialdea, A.; Moreno, M. A.; Escribano, R.; Herrero, V. J. Experimental Studies of Amorphous and Polycrystalline Ice Films Using FT-RAIRS. *J. Phys. Chem. B* **2003**, *107*, 11098−11108.
(16) Zondlo, M. A.; Onasch, T. B.; Warshawsky, M. S.; Tolbert, M. A.; Mallick, G.; Arentz, P.; Robinson, M. S. Experimental Studies of Vapor-Deposited Water-Ice Films Using Grazing-Angle FTIR-Reflection Absorption Spectroscopy. *J. Phys. Chem. B* **1997**, *101*, 10887−10895.
(17) Rudakova, A. V.; Poretskiy, M. S.; Marinov, I. L.; Tsyganenko, A. A. IR Spectroscopic Study of Surface Properties of Amorphous Water Ice. *Opt. Spectrosc.* **2011**, *109*, 708−718.
(18) Mitlin, S.; Leung, K. T. Surface Chemistry of OH Dangling Bonds in Vapour-Deposited Ice Films at 128−185 K. Hydrogen-Bonding Interactions with Acetone. *Surf. Sci.* **2002**, *505*, L227−L236.
(19) Schaff, J. E.; Roberts, J. T. Toward an Understanding of the Surface Chemical Properties of Ice: Differences Between the Amorphous and Crystalline Surfaces. *J. Phys. Chem.* **1996**, *100*, 14151−14160.
(20) Zimbitas, G.; Haq, S.; Hodgson, A. The Structure and Crystallization of Thin Water Films on Pt(111). *J. Chem. Phys.* **2005**, *123*, 174701/1−174701/9.
(21) Jenniskens, P.; Blake, D. F. Structural transitions in amorphous water ice and astrophysical implications. *Science (Washington, D.C.)* **1994**, *265*, 753−6.
(22) Jacobs, D. C. Reactive Collisions of Hyperthermal Energy Molecular Ions with Solid Surfaces. *Annu. Rev. Phys. Chem.* **2002**, *53*, 379−407.
(23) Cyriac, J.; Pradeep, T.; Kang, H.; Souda, R.; Cooks, R. G. Low-Energy Ionic Collisions at Molecular Solids. *Chem. Rev.* **2012**, *112*, 5356−5411.
(24) Bag, S.; Bhuin, R. G.; Natarajan, G.; Pradeep, T. Probing Molecular Solids with Low-Energy Ions. *Annu. Rev. Anal. Chem.* **2013**, *6*, 97−118.
(25) Cooks, R. G.; Ast, T.; Pradeep, T.; Wysocki, V. Reactions of Ions with Organic Surfaces. *Acc. Chem. Res.* **1994**, *27*, 316−323.
(26) Düerr, H.; Poker, D. B.; Zehner, D. M.; Barrett, J. H. Determination of the Reconstruction of Cu(110)-(2 × 3)-N with High-Energy Ion Scattering. *Phys. Rev. B: Condens. Matter* **1994**, *49*, 16789−16792.
(27) Bag, S.; McCoustra, M. R. S.; Pradeep, T. Formation of H_2^+ by Ultra-Low-Energy Collisions of Protons with Water Ice Surfaces. *J. Phys. Chem. C* **2011**, *115*, 13813−13819.
(28) Kolling, T.; Sun, S.; Weitzel, K.-M. Reactive Scattering of NH_3^+ (v, J) Ions at Film Covered Indium Tin Oxide (ITO) Surfaces. *Int. J. Mass Spectrom.* **2008**, *277*, 245−250.
(29) de, C. H. L.; Sen, A. D.; Shukla, A. K.; Futrell, J. H. Inelastic Ion-Surface Collisions: Scattering and Dissociation of Low Energy Benzene Molecular Cations. *Int. J. Mass Spectrom.* **2001**, *212*, 491−504.
(30) Herman, Z.; Mark, T. D. Collisions of Hydrocarbon Ions of Energies 10−50 eV with Carbon Surfaces: Ion Survival, Dissociation, Chemical Reactions, Scattering. *At. Plasma-Mater. Interact. Data Fusion* **2008**, *14*, 34−43.
(31) Qian, K.; Shukla, A.; Futrell, J. Electronic Excitation in Low-Energy Collisions: A Study of the Collision-Induced Dissociation of Nitromethane Ion by Crossed-Beam Tandem Mass Spectrometry. *J. Am. Chem. Soc.* **1991**, *113*, 7121−7129.
(32) Grill, V.; Shen, J.; Evans, C.; Cooks, R. G. Collisions of Ions With Surfaces at Chemically Relevant Energies: Instrumentation and Phenomena. *Rev. Sci. Instrum.* **2001**, *72*, 3149−3179.
(33) Shukla, A. K.; Futrell, J. H. Tandem Mass Spectrometry: Dissociation of Ions by Collisional Activation. *J. Mass Spectrom.* **2000**, *35*, 1069−1090.
(34) Cyriac, J.; Pradeep, T. Probing Difference in Diffusivity of Chloromethanes through Water Ice in the Temperature Range of 110−150 K. *J. Phys. Chem. C* **2007**, *111*, 8557−8565.
(35) Cyriac, J.; Pradeep, T. Interaction of Carboxylic Acids and Water Ice Probed by Argon Ion Induced Chemical Sputtering. *J. Phys. Chem. C* **2008**, *112*, 1604−1611.
(36) Cyriac, J.; Pradeep, T. Structural Reorganization on Amorphous Ice Films below 120 K Revealed by Near-Thermal (∼1 eV) Ion Scattering. *J. Phys. Chem. C* **2008**, *112*, 5129−5135.
(37) Benninghoven, A.; Sichtermann, W. K. Detection, Identification, and Structural Investigation of Biologically Important Compounds by Secondary Ion Mass Spectrometry. *Anal. Chem.* **1978**, *50*, 1180−1184.
(38) Benninghoven, A. Analysis of Monomolecular Surface Layers of Solids by Secondary Ion Emission. *Z. Phys.* **1970**, *230*, 403−417.
(39) Benninghoven, A.; Hagenhoff, B.; Niehuis, E. Surface MS: Probing Real-World samples. *Anal. Chem.* **1993**, *65*, 630A−640A.
(40) Leute, A.; Rading, D.; Benninghoven, A.; Schroeder, K.; Klee, D. Static SIMS Investigation of Immobilized Molecules on Polymer Surfaces. *Adv. Mater.* **1994**, *6*, 775−780.
(41) Trakhtenberg, S.; Naaman, R.; Cohen, S. R.; Benjamin, I. Effect of the Substrate Morphology on the Structure of Adsorbed Ice. *J. Phys. Chem. B* **1997**, *101*, 5172−5176.
(42) Chen, H.; Aleksandrov, A.; Chen, Y.; Zha, S.; Liu, M.; Orlando, T. M. Probing Water Interactions and Vacancy Production on Gadolinia-Doped Ceria Surfaces Using Electron Stimulated Desorption. *J. Phys. Chem. B* **2005**, *109*, 11257−11262.
(43) Herring, J.; Aleksandrov, A.; Orlando, T. M. Stimulated Desorption of Cations from Pristine and Acidic Low-Temperature Water Ice Surfaces. *Phys. Rev. Lett.* **2004**, *92*, 187602/1−187602/4.
(44) Kumar, G. N.; Cyriac, J.; Bag, S.; Pradeep, T. Low Energy Ion Scattering Investigations of n-Butanol-Ice System in the Temperature Range of 110−150 K. *J. Phys. Chem. C* **2009**, *113*, 14258−14263.
(45) Moon, E.-S.; Kang, H.; Oba, Y.; Watanabe, N.; Kouchi, A. Direct Evidence for Ammonium Ion Formation in Ice Through Ultraviolet-Induced Acid-Base Reaction of NH_3 with H_3O^+. *Astrophys. J.* **2010**, *713*, 906−911.
(46) Moon, E.-S.; Kang, H. Metastable Hydronium Ions in UV-Irradiated Ice. *J. Chem. Phys.* **2012**, *137*, 204704/1−204704/8.
(47) Kasi, S. R.; Kang, H.; Sass, C. S.; Rabalais, J. W. Inelastic Processes in Low-Energy Ion-Surface Collisions. *Surf. Sci. Rep.* **1989**, *10*, 1−104.
(48) Winters, H. F. Chemical Sputtering, a Discussion of Mechanisms. *Radiat. Eff.* **1982**, *64*, 79−79.
(49) Cooks, R. G.; Ast, T.; Mabud, M. A. Collisions of Polyatomic Ions with Surfaces. *Int. J. Mass Spectrom. Ion Processes* **1990**, *100*, 209−265.
(50) Materer, N.; Starke, U.; Barbieri, A.; Van, H. M. A.; Somorjai, G. A.; Kroes, G. J.; Minot, C. Molecular Surface Structure of Ice(0001): Dynamical Low-Energy Electron Diffraction, Total-Energy Calculations and Molecular Dynamics Simulations. *Surf. Sci.* **1997**, *381*, 190−210.
(51) May, R. A.; Smith, R. S.; Kay, B. D. Probing the Interaction of Amorphous Solid Water on A Hydrophobic Surface: Dewetting and Crystallization Kinetics of ASW on Carbon Tetrachloride. *Phys. Chem. Chem. Phys.* **2011**, *13*, 19848−19855.
(52) Beniya, A.; Koitaya, T.; Mukai, K.; Yoshimoto, S.; Yoshinobu, J. Dewetting Growth of Crystalline Water Ice on a Hydrogen Saturated Rh(111) Surface at 135 K. *J. Chem. Phys.* **2011**, *135*, 054702/1−054702/5.

(53) Beniya, A.; Sakaguchi, Y.; Narushima, T.; Mukai, K.; Yamashita, Y.; Yoshimoto, S.; Yoshinobu, J. The Growth Process of First Water Layer and Crystalline Ice on the Rh(111) Surface. *J. Chem. Phys.* **2009**, *130*, 034706/1−034706/10.
(54) Souda, R. Dewetting of Thin Amorphous Solid Water Films and Liquid-Cubic Ice Coexistence in Droplets Studied Using Infrared-Absorption and Secondary-Ion-Mass Spectroscopy. *J. Phys. Chem. B* **2008**, *112*, 11976−11980.
(55) Souda, R. Effects of Methanol on Crystallization of Water in the Deeply Supercooled Region. *Phys. Rev. B: Condens. Matter Mater. Phys.* **2007**, *75*, 184116/1−184116/7.
(56) Kimmel, G. A.; Petrik, N. G.; Dohnalek, Z.; Kay, B. D. Crystalline Ice Growth on Pt(111) and Pd(111): Nonwetting Nrowth on a Hydrophobic Water Monolayer. *J. Chem. Phys.* **2007**, *126*, 114702/1−114702/10.
(57) Smith, R. S.; Zubkov, T.; Dohnalek, Z.; Kay, B. D. The Effect of the Incident Collision Energy on the Porosity of Vapor-Deposited Amorphous Solid Water Films. *J. Phys. Chem. B* **2009**, *113*, 4000−4007.
(58) Stähler, J.; Mehlhorn, M.; Bovensiepen, U.; Meyer, M.; Kusmierek, D. O.; Morgenstern, K.; Wolf, M. Impact of Ice Structure on Ultrafast Electron Dynamics in D_2O Clusters on Cu(111). *Phys. Rev. Lett.* **2007**, *98*, 206105/1−206105/4.
(59) Mehlhorn, M.; Morgenstern, K. Faceting during the Transformation of Amorphous to Crystalline Ice. *Phys. Rev. Lett.* **2007**, *99*, 246101/1−246101/4.
(60) Du, Q.; Freysz, E.; Shen, Y. R. Surface Vibrational Spectroscopic Studies of Hydrogen Bonding and Hydrophobicity. *Science* **1994**, *264*, 826−828.
(61) Witek, H.; Buch, V. Structure of Ice Multilayers on Metals. *J. Chem. Phys.* **1999**, *110*, 3168−3175.
(62) Verdaguer, A.; Sacha, G. M.; Bluhm, H.; Salmeron, M. Molecular Structure of Water at Interfaces: Wetting at the Nanometer Scale. *Chem. Rev.* **2006**, *106*, 1478−1510.